

## Research Article

# Simulation Research on Safe Flow Rate of Bidirectional Crowds Using Bayesian-Nash Equilibrium

Can Liao <sup>1,2</sup>, Kejun Zhu,<sup>1</sup> Haixiang Guo <sup>1</sup> and Jian Tang<sup>1</sup>

<sup>1</sup>School of Management and Economics, China University of Geosciences, Wuhan 430074, China

<sup>2</sup>Katz Graduate School of Business, University of Pittsburgh, Pittsburgh, PA 15260, USA

Correspondence should be addressed to Can Liao; liaocan@cug.edu.cn and Haixiang Guo; ghx@cug.edu.cn

Received 29 September 2018; Revised 29 October 2018; Accepted 2 December 2018; Published 15 January 2019

Academic Editor: Jordi Duch

Copyright © 2019 Can Liao et al. This is an open access article distributed under the Creative Commons Attribution License, which permits unrestricted use, distribution, and reproduction in any medium, provided the original work is properly cited.

Current research on pedestrian flows has mainly focused on evacuation optimization during or after emergencies; however, crowd management before emergencies has received little attention. This paper examines the management of a Safe Pedestrian Flow Rate, in which the Bayesian-Nash Equilibrium mimics pedestrians' decision-making, and a multiagent system is employed to reproduce pedestrians' interactions. In the model, the pedestrian tunnel is divided into cells, with each pedestrian in a cell receiving a utility depending on the distance to the exit and the number of pedestrians in the cell. Then, each pedestrian uses the Bayesian-Nash Equilibrium to search for the target cell with maximum expected utility, moves in, and makes next decision until exiting the tunnel. The simulation model is calibrated and validated from a real scenario. Finally, from the experimental data collected from different simulation scenarios, this research reaches the conclusion that the Safe Pedestrian Flow Rate increases by about 2.96ped/s as the tunnel width expanded by 1m. This paper offers a novel method for reducing potential losses caused by crowd emergencies and can be a valuable reference for managing pedestrian flows and designing public places.

## 1. Introduction

As urbanization increases, urban populations worldwide have grown exponentially. As a result, stampede accidents such as the Shanghai New Year's Eve stampede in 2015, the Phnom Penh stampede in 2010, the Beijing Lantern Festival stampede in 2004, and the Mecca Hajj stampedes have become more frequent. According to incomplete statistics, over 100 stampede accidents have occurred since 2001, causing more than 10,000 deaths [1]. Therefore, research on pedestrian flows, especially in dense situations, has become a more important research focus.

However, as current crowd research mainly focused on evacuation optimization after an emergency, the management of pedestrian flows before an emergency received little attention. From the two photographs in Figure 1, it can be seen that as roads or venues are always crowded with pilgrims or pedestrians moving in opposite directions during ceremonies and holidays, accidents or near accidents can easily occur. Therefore, studies on managing pedestrian flows

to prevent or control stampedes or other emergencies are required.

In this paper, a model is developed to mimic pedestrian crowd decision-making and determine a Safe Pedestrian Flow Rate (SPFR) for different situations. The remainder of this paper is organized as follows. Section 2 gives a brief review of previous research on pedestrian flows. Section 3 introduces the proposed simulation model in detail, including the decision-making processes and the collision avoidance strategies. Section 4 calibrates and validates the model with data collected from an actual scene. Section 5 conducts simulation experiments that consider pedestrians' walking preferences under different circumstances and reveals the relationships between the SPFR and the tunnel width. Section 6 concludes the work and discusses prospects for future research.

## 2. Literature Review

When analyzing an emergency, the period can be divided into three phases: before emergency, during emergency,



(a) The Duanqiao Bridge in Hangzhou

(b) The Bund Park in Shanghai

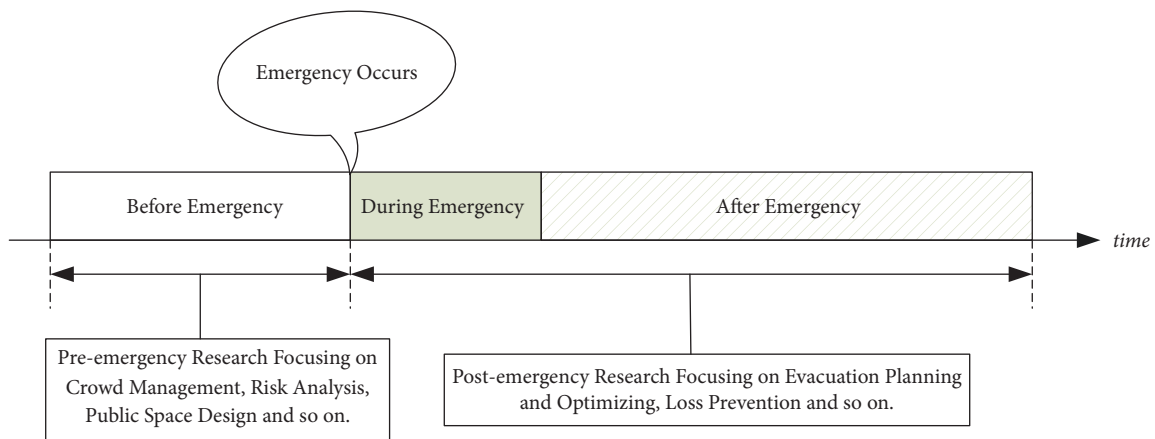
FIGURE 1: Scenarios for pilgrims/tourists ((a) is downloaded from <http://www.163.com>, and (b) is downloaded from <https://baike.baidu.com/>).

FIGURE 2: Definition of pre-emergency research and post-emergency research.

and after emergency. This paper classifies current emergency research into two pre-emergency research and post-emergency research, as shown in Figure 2. Generally, pre-emergency research focuses on the work before emergencies happen, such as crowd management, risk analysis, and public space design, while post-emergency research keeps an eye on the work during or after emergencies happen, such as evacuation planning and optimizing and loss prevention.

Present pedestrian flow models can be divided into macroscopic and microscopic models. Macroscopic models examine overall pedestrian flows and research pedestrian characteristics using qualitative theories or methods from other disciplines, such as the Fluid Dynamics Model proposed by Huges [2, 3] and Wave Theory introduced by Lu [4]. Microscopic models, on the other hand, such as the Lattice Gas Model [5], the Social Force Model [6, 7], the Cellular Automata Model [8, 9], and the Agent-based Model [10, 11], focus on the influence of individual behavior on pedestrian flows. As macroscopic models study overall pedestrian flows and ignore the heterogeneity and complexity of individuals, they are unable to accurately analyze the mechanisms between the microscopic pedestrian behavior and the macroscopic phenomena of the crowd. Therefore, microscopic models have been the main methods used for

pedestrian flow research [12–15]. Table 1 summarizes recent research on pedestrian flows.

From Table 1, it can be seen that nearly 75% of recent research has been focused on post-emergency, such as reproducing evacuation scenes and optimizing evacuations, with very few examining situations before the crises occurred. What is more, as most pre-emergency research has focused on the reproduction of pedestrian flow phenomena and the optimization of emergency plan, crowd management to avoid accidents has received very little research attention. Further, while many studies have examined the factors that influence egress efficiency, neither the quantitative nor concrete relationships between these factors have been explored. The common characteristic in current research has been that almost all authors have employed a methodology that combined at least two modeling methods, with one being a decision or behavioral model that mimics pedestrians' decision-making or behaviors and the other being an action model that motivates pedestrians' movement.

The main purpose of this research, therefore, is to determine a scientific, practical method for managing crowds at a safe level to prevent possible emergencies. Game theory has been found to be able to properly capture a pedestrian's decision-making processes and interactions, and agent-based

TABLE 1: Brief summary of recent studies on pedestrian flow.

Article	Methodology	Focus of Research	Pre-emergency /Post-emergency
[10]	Visual intelligence & AB	Estimate evaluation time	Pre-emergency
[11]	Decision support system & AB	Safety evaluation	Pre-emergency
[16]	Artificial Neural Network	Route choice behavior	Pre-emergency
[17]	Combination of macroscopic model and microscopic model	Prediction of evacuation time	Pre-emergency
[18]	Fuzzy logic& microscopic simulation	Model research	Pre-emergency
[19]	Multi-grid method & CA	Characteristics of unidirectional pedestrian flows	Pre-emergency
[20]	Toy model & microscopic simulation	Bidirectional pedestrian flow	Pre-emergency
[21]	Improved CA	Walking Strategies of Bidirectional Pedestrians	Pre-emergency
[22]	Monte-Carlo simulation & Game Theory	Pedestrian Group-Crossing Behavior	Pre-emergency
[6]	Modified social force model	Influence of information transmission	Post-emergency
[8]	Improved cellular automaton model	Influence of route changes and group fields	Post-emergency
[23]	GA & microscopic pedestrian simulation	Optimal evacuation plan	Post-emergency
[24]	Game theory & CA	Influence of cooperation and psychological factors	Post-emergency
[25]	Local optimal decision & SF	Evacuations	Post-emergency
[26]	Game theory & AB	Model research	Post-emergency
[27]	Experiments & improved force-based model simulation	Impact of vision on uni- and bi-directional flows	Post-emergency
[28]	Experimental study	Relationship between crowd density and crawling movements	Post-emergency
[29]	Surveys, evacuation experiments & statistical analyses	Exit choices for pedestrian crowd evacuees	Post-emergency
[30]	Improved cellular automaton model	Group Influence	Post-emergency
[31]	Probabilistic model & Latin Hypercube Sampling method	Evacuation safety evaluation	Post-emergency
[32]	Evolving network & CA	Decision-making process and cooperative behavior	Post-emergency
[33]	Fuzzy theory & LG	Influence of information transmission on crowds	Post-emergency
[34]	Grouping algorithm & SF	Influence of Groups	Post-emergency
[35]	Cost potential field & CA	Influence of behavior variations	Post-emergency
[36]	Driving-forces model & AB	Influence of moving threats	Post-emergency
[37]	Improved cellular automaton model	Effect of psychological tension	Post-emergency
[38]	Empirical study	Influence of social groups	Post-emergency
[39]	Route learning method & modified social force model	Factors for evacuation efficiency	Post-emergency

In the table, AB is short for agent based model, CA is short for cellular automata model, LG is short for lattice gas model, and SF is short for social force model.

modeling methods have been proven to effectively mimic pedestrian movements [13]. This paper, therefore, adopts a multiagent system and the Bayesian-Nash Equilibrium to formulate the simulation model. In the model, one or more pedestrians are permitted to stay in a cell, with each pedestrian assigned a utility that depends on their distance to the exit and the number of other pedestrians sharing the cell. The Bayesian-Nash Equilibrium is an equilibrium achieved in incomplete information games in which each player chooses a strategy to gain a maximum expected

utility based on the probability distributions of the others' decisions. The simulation experiment in this model is self-organized once it begins to run, as the pedestrian does not know the exact choices their neighbors are going to make. They choose a target cell to gain as much utility as possible based on the probability distributions of the neighboring pedestrians' choices. Hughes pointed out that emergencies can easily occur when pedestrian density is greater than  $4\text{ped}/\text{m}^2$  [2]; therefore, this paper regards the density of  $4\text{ped}/\text{m}^2$  to be the Critical Emergency Density and defines the

TABLE 2: Main pedestrian flow measures.

Full Name	Abbreviation	Meaning
Critical Density (Ped/m <sup>2</sup> )	-	Threshold density at which emergencies could occur.
Pedestrian Flow Rate (Ped/s)	-	The average number of pedestrians passing by in a time unit
Safe Pedestrian Flow Rate (Ped/s)	SPFR	Maximal pedestrian flow rate to avoid exceeding the critical pedestrian density
Velocity of Pedestrian Flow (m/s)	VPF	Average speed of all the pedestrians at one time, to determine the real-time pedestrian flow speed.
Average Velocity of Pedestrian Flow (m/s)	AVPF	Average VPF from the beginning of the experiment to the end, which is used to indicate the pedestrian flow efficiency in a specific scenario.

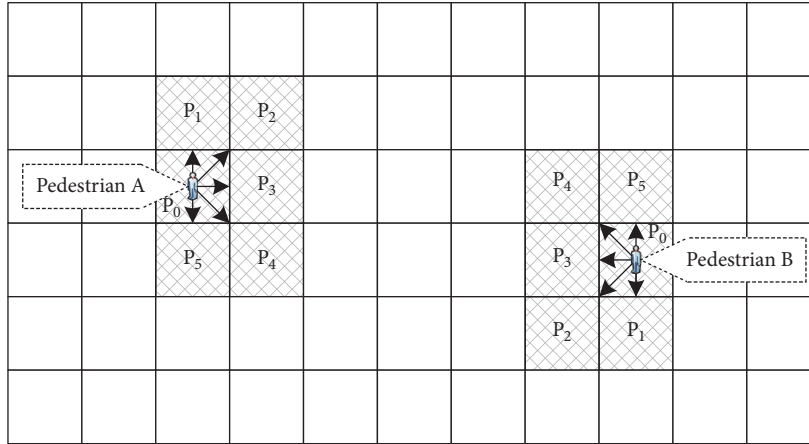


FIGURE 3: Probabilities of the target cell being chosen by pedestrians when walking in different directions.

maximal pedestrian flow rate before the critical density as the Safe Pedestrian Flow Rate (*SPFR*). In other words, if timely measures are not taken when the pedestrian flow exceeds the *SPFR*, it is more likely that an emergency could occur. To be clear, the main pedestrian flow measures in this paper are as shown in Table 2.

### 3. Simulation Model Framework

**3.1. Initial Model Environment.** This paper studies pedestrian flows using Agent-Based Modeling and Simulation (ABMS). Pedestrians enter the pedestrian tunnel from both ends and walk in two opposite directions: left to right and right to left; as shown in Figure 3, and as with most models, the tunnel is divided into cells. In most existing microscopic models, the evacuation venues are partitioned into square (diamond, or hexagon) cells with 0.4m sides, which are based on pedestrian projections. In other words, these models cannot simulate pedestrians density more than  $1\text{ped}/(0.4\text{m}\times 0.4\text{m})$ , which is about  $6\text{ped}/\text{m}^2$ . What is more, when the pedestrian moves from one cell to another, the distance is not in accordance with the actual average pedestrian walking step length. When the pedestrian moves more than one cell in each time step, their decision-making processes become rather complex as many factors need to be considered, such as decision-making efficiency and the target cell's availability.

Based on experimental data and statistical analyses, Zeng determined that in a normal condition a pedestrian walks with a step length of 0.7m and at a speed of 1.4m/s [40]. This paper, therefore, sets the side length of the cell at 0.7m based on the average pedestrian step length, with pedestrians making decisions every 0.5s. In other words, at each second the pedestrian moves twice and moves no more than one cell each time. The probability that a pedestrian chooses each target cell is shown in Figure 3.

In Figure 3, Pedestrian A and Pedestrian B are pedestrians walking from left to right and from right to left,  $p_1$ ,  $p_2$ ,  $p_3$ ,  $p_4$ , and  $p_5$  are the successive probabilities of the adjacent cells being chosen by the pedestrian from their left side to right side, and  $p_0$  is the probability that a pedestrian remains stationary.

**3.2. Utility Function.** The utility that a pedestrian gains while walking depends on their desire to achieve their destination [35]. In this research, the utility is divided into movement utility  $\mu_{move}$  and comfort utility  $\mu_{comf}$ , as follows.

$$\mu = \mu_{move}(s, \theta) + \mu_{comf}(n) \quad (1)$$

The movement utility depends on the distance the pedestrian moves toward to the exit and is defined as

$$\mu_{move}(s, \theta) = s \times \cos \theta \quad (2)$$

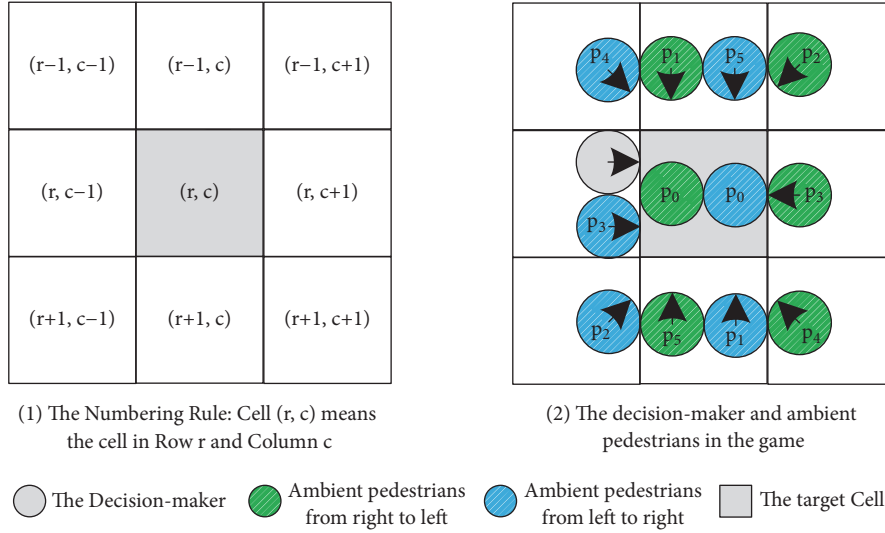


FIGURE 4: Pedestrians in the game. (1) demonstrates the cell numbering rule. (2) illustrates how ambient pedestrians affect the decision-maker's expected comfort utility.

where  $s$  is the distance the pedestrian moves each time and  $\theta$  is the angle between the movement direction and the exit direction. For example, when a pedestrian walks straight to the exit,  $\theta$  equals 0 and when they walk in a vertical direction to the exit,  $\theta$  equals 90.

A relationship has been found between the pedestrian's speed and crowd density; however, few studies have developed a formula for this relationship. Zeng summarized former studies and provided a function for pedestrian velocity: pedestrians are able to move freely if the density is below  $4\text{ped}/\text{m}^2$ , have severely restricted movements when the density exceeds  $7\text{ped}/\text{m}^2$ , and when the density is between  $4\text{ped}/\text{m}^2$  and  $7\text{ped}/\text{m}^2$ , the pedestrian has restricted velocity, which is related to the density [40]. Based on the function, this paper defines 1.00 as the pedestrian comfort utility when they can move freely, with the ratio of restricted speed to free speed being their comfort utility value in other cases, as follows.

$$\mu_{\text{comf}}(n) = \begin{cases} 1.00, & n \leq 2 \\ 0.52, & n = 3 \\ 0.28, & n \geq 4 \end{cases} \quad (3)$$

where  $n$  denotes the number of pedestrians in the same cell.

**3.3. Expected Comfort Utility.** Pedestrians in the model do not know the other pedestrians' decisions, which could affect their own comfort utility, and therefore make independent decisions when walking. That is, before moving, each pedestrian has to calculate the expected utility of every possible decision based on the probability distribution of the other pedestrians' choices, after which they choose the cell with the maximum utility as the target cell. In this paper, a pedestrian is assumed to choose the target cell from six possible cells,

as shown in Figure 3, and each of the six alternative cells has eight neighboring cells, which means that many pedestrians may choose the same target cell, as shown in Figure 4.

Subgraph (1) in Figure 4 shows the cell numbering rule. Specifically, cell (r, c) denotes the cell in Row r Column c. Subgraph (2) illustrates the game interactions between the decision-maker and their neighboring pedestrians. The circles represent the pedestrians who may potentially choose Cell (r, c). Further, blue circles indicate pedestrians walking from left to right, and green ones denote pedestrians walking from right to left. It can be seen in subgraph (2) that the ambient pedestrians impact the expected comfort utility of the decision-maker in Cell (r, c-1) who chooses Cell (r, c) as their target cell. This means the decision-maker must consider the choices made by its surrounding pedestrians. Expressions in each circle represent the possibilities of pedestrians moving into the Cell (r, c) separately, according to Figure 3.

Take the decision-maker in Figure 4 as an example. As in the simulation model, a pedestrian should take all the situations into consideration before making a decision. Thus, a pedestrian's expected utility of the target cell can be divided into four parts, which are utility of one pedestrian, of two pedestrians, of three pedestrians, and of more than three pedestrians. The expected comfort utility  $\xi_{\text{comf}}$  is

$$\begin{aligned} \xi_{\text{comf}} = & \mu_{\text{comf}}(1) p(0) + \mu_{\text{comf}}(2) p(1) \\ & + \mu_{\text{comf}}(3) p(2) \\ & + \mu_{\text{comf}}(4) [1 - p(0) - p(1) - p(2)] \end{aligned} \quad (4)$$

where  $p(0)$ ,  $p(1)$ ,  $p(2)$  represent the possibility of no pedestrians, one pedestrian, or two pedestrians in Cell (r, c), respectively.

In this paper,  $n_{r,c}^r$  is used to denote the number of pedestrians in Cell (r, c) walking from left to right, and  $n_{r,c}^l$  is used to denote the number of pedestrians in Cell

(r, c) walking from right to left. According to Figure 4, ambient pedestrians can be divided into six groups based on the possibility of moving into Cell (r, c); the numbers of pedestrians in each group are  $n_{r,c}^l + n_{r,c}^r$ ,  $n_{r-1,c}^l + n_{r+1,c}^r$ ,  $n_{r-1,c+1}^l + n_{r+1,c-1}^r$ ,  $n_{r,c+1}^l + n_{r,c-1}^r - 1$ ,  $n_{r+1,c+1}^l + n_{r-1,c-1}^r$ , and  $n_{r+1,c}^l + n_{r-1,c}^r$ , which are replaced with  $g_0, g_1, g_2, g_3, g_4, g_5$  for convenience. The corresponding possibilities for pedestrians in each group moving into Cell (r, c) are  $p_0, p_1, p_2, p_3, p_4, p_5$ .

The probability that no pedestrians choose Cell (r, c) is

$$p(0) = \prod_{i=0}^5 (1 - p_i)^{g_i} \quad (5)$$

and the probability that only one pedestrian chooses Cell (r, c) is

$$p(1) = \sum_{i=0}^5 \frac{g_i p_i p(0)}{1 - p_i} \quad (6)$$

When two pedestrians choose the target cell, they may come from the same group or two different groups, in which case, it could be calculated separately.

$$p(2) = p'(2) + p''(2) \quad (7)$$

If the two pedestrians come from the same group,

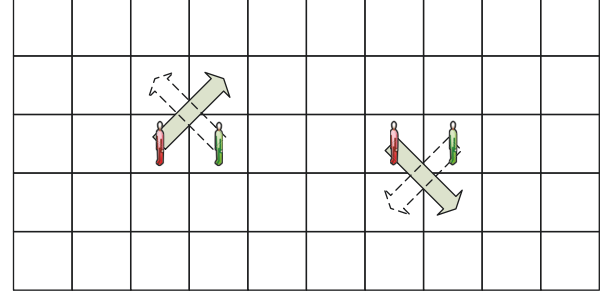
$$p'(2) = \sum_{i=0}^5 \frac{g_i (g_i - 1)}{2} \frac{p_i^2 p(0)}{(1 - p_i)^2} \quad (8)$$

and if they come from two different groups,

$$\begin{aligned} p''(2) &= \sum_{i=1}^5 \frac{g_0 g_i p_0 p_i p(0)}{(1 - p_0)(1 - p_i)} + \sum_{i=2}^5 \frac{g_1 g_i p_1 p_i p(0)}{(1 - p_1)(1 - p_i)} \\ &+ \sum_{i=3}^5 \frac{g_2 g_i p_2 p_i p(0)}{(1 - p_2)(1 - p_i)} + \sum_{i=4}^5 \frac{g_3 g_i p_3 p_i p(0)}{(1 - p_3)(1 - p_i)} \\ &+ \sum_{i=5}^5 \frac{g_4 g_i p_4 p_i p(0)}{(1 - p_4)(1 - p_i)} \end{aligned} \quad (9)$$

When a pedestrian chooses other cells or is at other positions, the method used to calculate their expected comfort utility is the same. Further, to keep pedestrians in the tunnel, the expected comfort utility is defined as negative infinity when the target cell is beyond the upper or the lower boundaries.

**3.4. Collision Avoidance Action.** In most microscopic models, conflicts occur when pedestrians make decisions or move at the same time, as each cell can contain only one pedestrian. If conflicts are not properly dealt with in the model, pedestrians will go directly through other pedestrians or some other uncontrollable phenomena will occur, which inevitably leads to a false conclusion. This paper allows two or more pedestrians to share a cell and as a result avoids conflicts caused by pedestrians making simultaneous decisions; however, when





 Pedestrians walking from left to right  
 Pedestrians walking from right to left

FIGURE 5: Collisions when pedestrians move simultaneously.

two or more pedestrians move at the same time, once their routes intersected, these collisions are still unavoidable in the model, as shown in Figure 5.

As we all know, collisions seldom happen even in extremely dense crowds because pedestrians can generally perceive possible collisions before happening and immediately change their routes. This paper, therefore, makes a rule that if a collision is likely to happen, each of the involved pedestrians changes their decisions to an adjacent alternative cell with a chance of  $p_{avoi}$ . Based on the above collision definition, it can be concluded that collisions can only occur between pedestrians moving in opposite directions, as shown in Figure 5. For instance, a pedestrian in Cell (r, c-1) walking from left to right predicts a collision only when they choose Cell (r-1, c) or Cell (r+1, c) and if there are pedestrians in Cell (r, c) walking from right to left. It is important to note that even if the pedestrian in Cell (r, c-1) does not change their decision, there is still a chance that a collision does not occur as pedestrians in Cell (r, c) may not choose the same cell. From this point of view, the chance that a pedestrian changes their minds to avoid a collision should be approximated to the possibility that a collision may occur. In this research,  $p_{avoi}$  is defined as follows:

$$\begin{aligned} p_{avoi} &= \begin{cases} 1 - (1 - p_4)^{n_{r,c}^l}, & \text{when choosing Cell (r-1, c)} \\ 1 - (1 - p_2)^{n_{r,c}^r}, & \text{when choosing Cell (r+1, c)} \end{cases} \end{aligned} \quad (10)$$

where  $n_{r,c}^l$ ,  $p_2$ , and  $p_4$  are in accordance with previous sections.

**3.5. Decision-Making Process.** The detailed process for the pedestrians' decision-making is shown in Figure 6. In each time step, a pedestrian calculates its utilities of all available choices. After that, it chooses the cell with maximal expected utility as its target cell. Then it takes an action to avoid possible collisions. Finally, it moves into the chosen cell and begins the next decision-making round until passing through the tunnel.

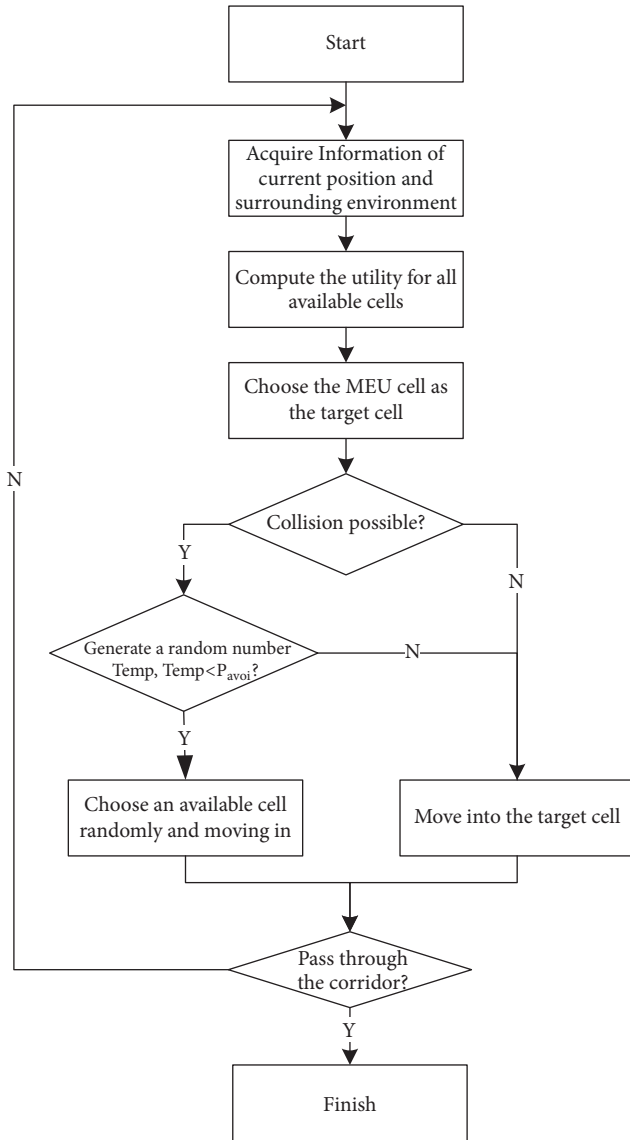


FIGURE 6: Pedestrian decision-making flow chart.

Before simulation, the length and the width of the tunnel, the pedestrian flow rate, and the probabilities from  $p_0$  to  $p_5$  are put into the model to initialize the experimental environment. During simulation, each pedestrian agent makes decisions according to the flow chart. After simulation, experimental data, such as the real-time velocity and real-time pedestrian distribution, are collected and analyzed.

## 4. Running the Simulation

**4.1. Parameters Initialization.** The simulation is based on data collected from a real tunnel about 300m long and 10m wide with a 12ped/s peak pedestrian flow. The peak of pedestrian flow lasts about 15 minutes. Over 10 gigabytes of videos on pedestrian movements is collected from the monitoring system. Through statistical analyzing, the possibilities of each alternative cell being chosen by the pedestrians are found

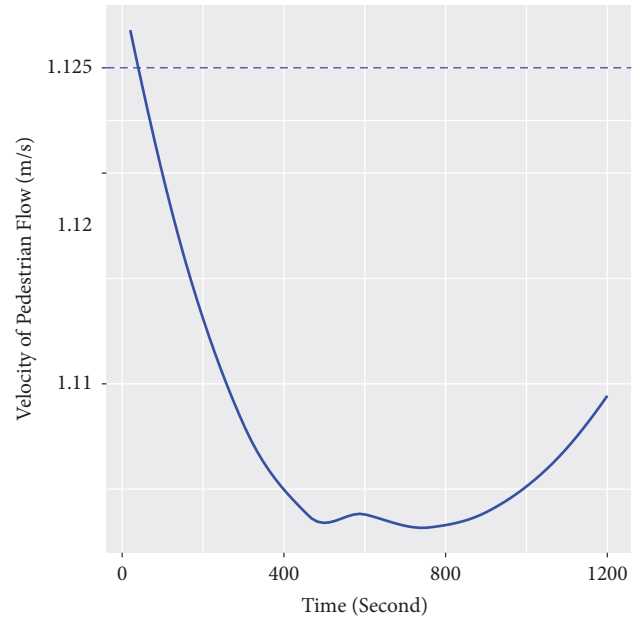


FIGURE 7: Transformation of the Velocity of Pedestrian Flow over time (The dashed line represents measured data in the real situation and the fitting curve shows experimental data in the simulation).

to be  $p_0 = p_4 = 0.1$ ,  $p_1 = p_3 = 0.2$ ,  $p_2 = 0.35$ ,  $p_5 = 0.05$  on average. After the simulation begins, the pedestrians walk into the tunnel from either of the two ends, and experimental data are collected and analyzed after 1200 seconds (20 minutes) to identify characteristics of the pedestrian flow in the tunnel. The detailed input parameter is listed in Table 3.

**4.2. Model Calibration and Validation.** An important pedestrian flow indicator, the Velocity of Pedestrian Flow (VPF), is defined as the average speed of all pedestrians in the tunnel at the same time. In Figure 7, the red dashed line stands for the actual average speed of pedestrians passing through tunnel, which is about 1.125m/s, while the blue fitting curve represents the VPF transformed over time in simulation. Though the model assigned an initial speed of 1.4m/s to each pedestrian (0.7m each step and two steps each second), it can be found from the experimental data that overall the pedestrians pass through the tunnel at a speed of around 1.11m/s. Considering the measurement error, it can be concluded that the VPF in the simulation experiment agrees with the real situation.

Figure 8 demonstrates the number of pedestrians getting out of tunnel over time, with circles representing data of real situation and the blue curve representing data of simulation. Each circle stands for the average number of pedestrians in a minute. It can be found that the peak number of pedestrians getting out of tunnel highly accords with the real situation. From Figures 7 and 8, it can be concluded that the proposed model can effectively mimic the bidirectional pedestrian flow.

TABLE 3: Parameters of the simulation.

Name	Value
Tunnel length	300m
Tunnel width	10m
The peak rate of pedestrian flow	12 ped/s
The time that pedestrian flow peak last	15 minutes
Simulation time	20 minutes
The possibilities of each alternative cell being chosen by the pedestrians $\{p_0, p_1, p_2, p_3, p_4, p_5\}$	$\{0.05, 0.10, 0.20, 0.35, 0.20, 0.10\}$

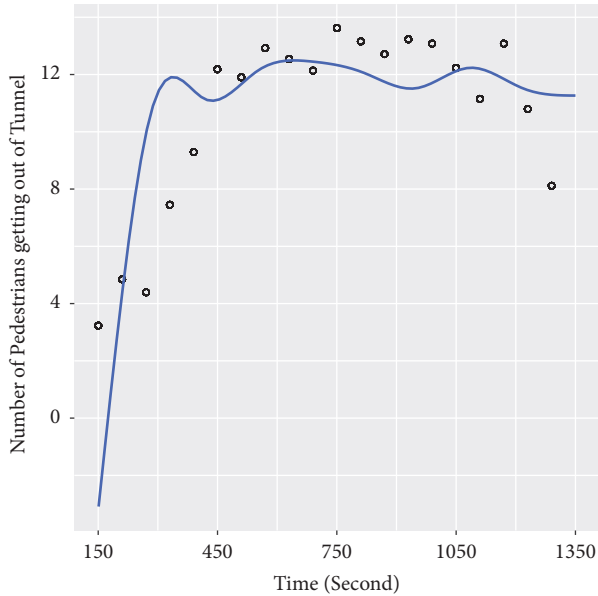


FIGURE 8: Number of pedestrians getting out of tunnel varies over time (circles show data collected from tunnel and the blue curve shows data collected from simulation).

**4.3. Simulation Experiments in Different Scenarios.** After calibrating and validating the model, experiments are conducted in several different scenarios to explore different circumstances. The Average Velocity of Pedestrian Flow (AVPF) is the average VPF from the beginning of the experiment to the end and reflects the efficiency of the pedestrian flow in the tunnel. To ensure the result's correctness, simulation experiments terminate after 3600 seconds (an hour) when researching the Safe Pedestrian Flow Rate.

To study the factors that influence the AVPF, experiments in scenarios with different tunnel lengths, different tunnel widths, and different pedestrian flow rates are conducted, and the results are shown in Figure 9. There are nine subgraphs in Figure 9, each with a layout of three rows and three columns. The left to right subgraphs in the three columns are the results for tunnel widths of 3m, 5m, and 10m, while the top to bottom subgraphs in the three rows show the experimental results for tunnel lengths of 100m, 200m, and 300m (this research has conducted experiments in various scenarios, such as different tunnel lengths (under 100m, exceeding 300m), different tunnel widths (under 3m, exceeding 10m),

different rates of pedestrian flow (under 3ped/s, exceeding 12ped/s), and has gotten similar results. This paper chooses data collected in some typical scenarios to display). The line in each subgraph indicates the AVPF changing with the pedestrian flow increasing from 3ped/s to 12ped/s in each scenario.

It can be seen from Figure 9 that subgraphs in the same column have few differences, indicating that the tunnel length has limited effect on the AVPF; however, as lines varied across the same row, the tunnel width is found to have a significant influence on the AVPF; that is, the AVPF increases as the width broadened. Curves in each subgraph decrease as the pedestrian flow rate increases; therefore, it can be surmised that the wider the tunnel is, the weaker the influence of pedestrian flow rate has on the AVPF. In summary, the simulations indicate that the tunnel width and the pedestrian flow rate significantly affect the AVPF, while tunnel length has limited influence.

It is a common sense that the greater the pedestrian density is, the more dangerous the space will be. As the model allows more than one pedestrian to stand in a cell, potential risk will increase with the number of pedestrians in a cell growing. This research collects real-time data of pedestrian distribution in the tunnel throughout experiments and the average data for the pedestrian distributions in different scenarios during experiments are displayed in Figure 10.

In accordance with Figure 9, subgraphs in Figure 10 show average pedestrian distributions with different tunnel lengths, different tunnel widths, and different pedestrian rates. In each subgraph, there are five differently colored bars, which represent the percentages of cells containing zero pedestrians, one pedestrian, two pedestrians, three pedestrians, and over three pedestrians. From a comparative analysis, it is concluded that tunnel length has a limited impact on pedestrian distribution, but tunnel width has a significant influence. Concretely, the proportion of multipedestrian cells increases while the tunnel width narrows down, and in certain tunnels, the ratio of cells containing multiple pedestrians increases with the pedestrian rate. Besides, it can be found that, except for the extreme conditions (3m wide tunnel with 12ped/s), the percentage of cells containing more than three pedestrians is below 5%, which indicates that pedestrians in the simulation are under tolerable situations (pedestrian density under 9ped/m<sup>2</sup>) [2].

As tunnel length is found to have limited impact on pedestrian flow movements, experiments are conducted



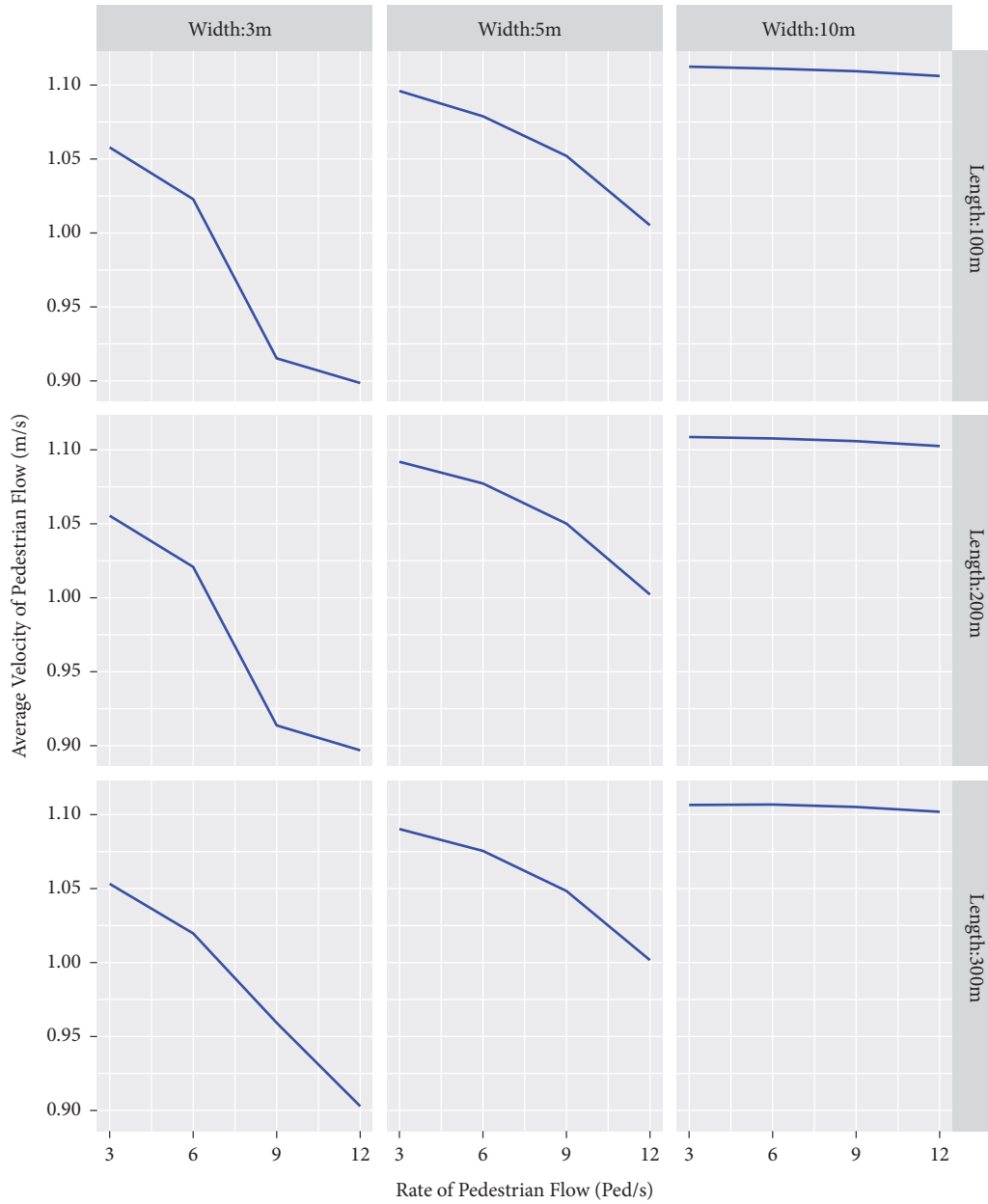


FIGURE 9: Average pedestrian flow velocities in different scenarios.

using a fixed tunnel length of 100m. Experimental data are collected in scenarios with different tunnel widths and different pedestrian flow rates. Figure 11 shows the average pedestrian density from the start to the completion of each experiment. The three lines in the figure, respectively, illustrate the average density transferring with the pedestrian rate when the tunnel widths are, respectively, 3m, 5m, and 10m. From the experimental data, it is found that tunnel width and pedestrian flow rate have significant influences on average density. Therefore, based on the critical density definition ( $4\text{ped}/\text{m}^2$ ), the SPFR is a function of tunnel width; that is, under certain circumstances, the SPFR is only related to tunnel width.

Through the many simulation experiments, SPFRs are collected under different scenarios, the fitting curve for which is shown in Figure 12, and the function is as follows:

$$y = 2.9643x - 1.0333 \quad (11)$$

where  $y$  is the SPFR and  $x$  is the tunnel width. We thus conclude that the SPFR has a linear relationship with tunnel width. Specifically, the SPFR increases by  $2.96\text{ped}/\text{s}$  as the tunnel width is expanded by  $1\text{m}$ , which can be useful information for managing pedestrian flows and designing public places.

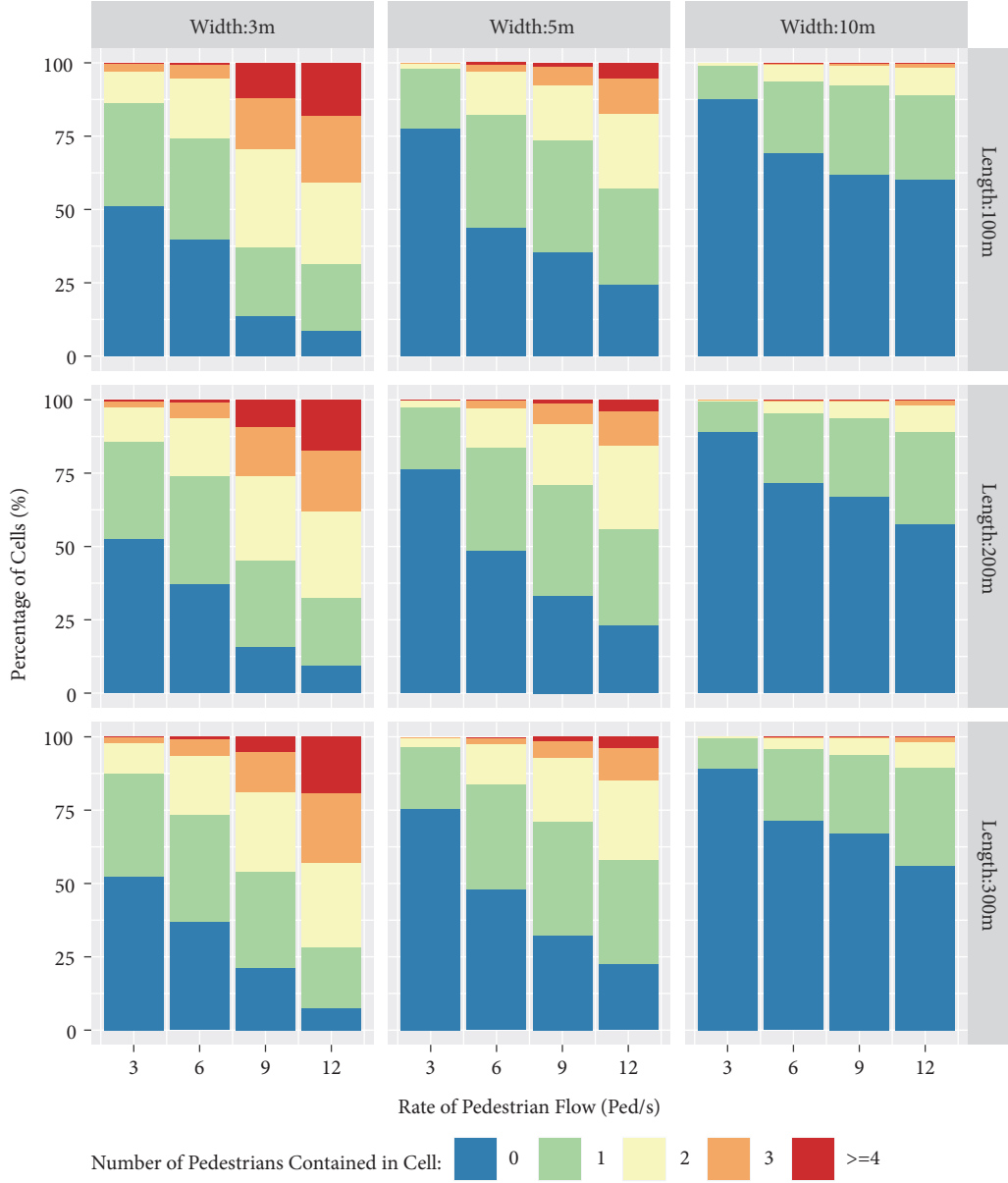


FIGURE 10: Pedestrian flow distributions in different scenarios.

## 5. Simulation Experiments with Walking Preferences

**5.1. Improved Simulation Model.** In the former experiments, pedestrians use the Bayesian-Nash Equilibrium to estimate their expected utility for each choice. After that they take collision avoidance actions before moving into their chosen cells. However, pedestrians usually have preferences when making their own decisions; for example, pedestrians in China usually walk in the right while in Japan, they walk in the left. Further, adults tend to move forward, while children are more likely to move around. Therefore, even in the same situations, different pedestrians will make different decisions based on their preferences. As walking preferences affect pedestrian decisions, which may affect the pedestrian flow,

the model is improved to study in depth the influence of microscopic walking preferences on macroscopic pedestrian flows.

A weight coefficient set  $\omega$  is employed to illustrate pedestrian walking preferences; when a pedestrian makes their preferred choice, their comfort utility is  $\omega$  times the previous. In the improved model, the total utility that a pedestrian expects to gain is defined as

$$\mu'_i = \mu_{mi} + \omega_i \xi_{ci} \quad (12)$$

where  $i$  is the serial number of the six choices, in which the numbering rule is in accordance with the possibility  $p$  in Figure 3,  $\mu'_i$  denotes the total expected utility of choice  $i$ ,  $\mu_{mi}$  and  $\xi_{ci}$ , respectively, are the expected movement utility and the comfort utility, and  $\omega_i$  denotes the pedestrian preference

TABLE 4: Weight coefficient set in each scenario.

Scenario	The weight coefficient set
Comparison Scenario (No Walking Preference)	$\omega_0 = \omega_1 = \omega_5 = 1.0, \omega_2 = \omega_3 = \omega_4 = 1.0;$
Experimental Scenarios (Forward walking Preferences)	$\omega_0 = \omega_1 = \omega_5 = 1.0, \omega_2 = \omega_3 = \omega_4 \sim N(\omega_f, 0.1^2);$

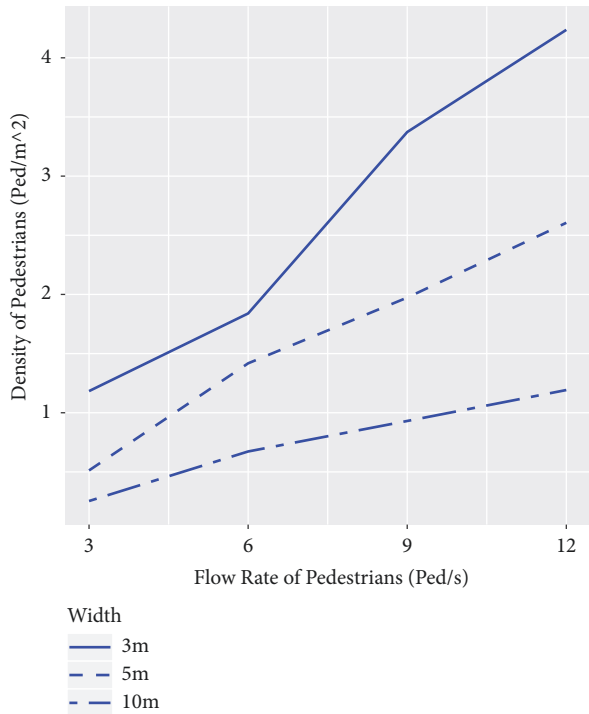


FIGURE 11: Pedestrians' density transformation over the pedestrian flow rate in the different scenarios.

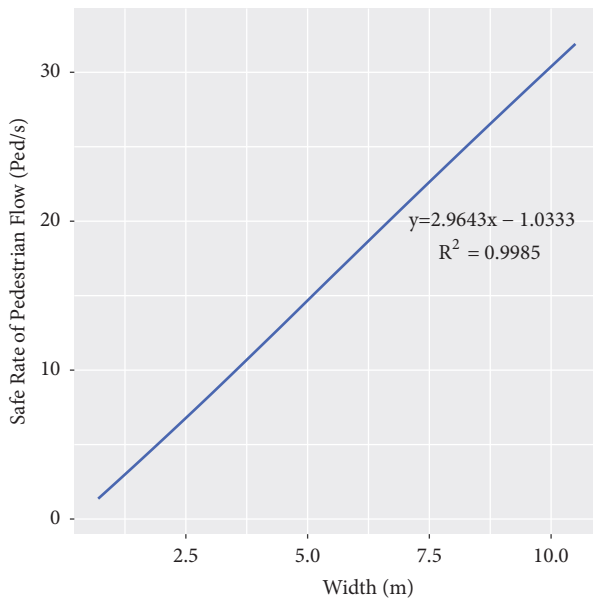


FIGURE 12: Safe pedestrian flow rate varying over tunnel width.

degree for choice  $i$ . The two subgraphs in Figure 13 show the expected comfort utilities with and without walking preferences for pedestrians walking from left to right. By adjusting the weight coefficients, the walking preferences that affect pedestrian flow are examined in this research.

**5.2. Simulation with Walking Preference.** Based on the improved model, experiments are conducted with forward walking preferences and right walking preferences; the tunnel in each experiment is 100m, the width is 10m, and the rate of pedestrian flow entering the tunnel from both ends is 12ped/s in total.

*(1) Forward Walking Preference.* When a pedestrian is eager to move out of a tunnel, they tend to prefer cells in front. Therefore, to examine effects of forward walking preferences on pedestrian flow, comparative experiments in different scenarios are conducted. The weight coefficient set  $\omega$  combinations for each scenario are shown in Table 4.

As different pedestrians may have different forward walking preferences, in the experimental scenarios the pedestrian preference degrees for cells in front are expected to obey a normal distribution with a mean value  $\omega_f$  and a standard deviation 0.1. It can be found that the pedestrian preference degree for the cells in front increases with  $\omega_f$ , and the number of pedestrians choosing the front cells increases as well. Figure 14 demonstrates the relationship between the AVPF and  $\omega_f$ .

From Figure 14, it can be observed that the AVPF is about 1.1m/s when pedestrians have no forward walking preferences; however, when  $\omega_f \leq 1.2$ , the AVPF increases with  $\omega_f$  and decreases when  $1.2 \leq \omega_f \leq 1.6$ . This is mainly because the pedestrian's desire to exit the tunnel increases, resulting in the pedestrians' distribution becoming uneven, and more pedestrians have to take collision avoidance actions, which in turn slow down the AVPF. When  $\omega_f \geq 1.6$ , the AVPF is stable at around 1.0m/s, which indicates that excessive forward walking preferences decrease the AVPF. The experiment indicates that a slight forward walking tendency promotes the pedestrian flow's movement, which can be used to improve pedestrian flow's efficiency in tunnels.

*(2) Right Walking Preference.* Note that the right in the walking direction of "from left to right" is relative to the tunnel, while in the "right-moving preference" it is relative to the pedestrians themselves. As mentioned, pedestrians in some areas prefer walking in the right, while in other areas they prefer walking in the left. The right walking pedestrian is taken as an example to examine the effect of side preferences on pedestrian flow. Note that naturally a pedestrian's right walking preference is no more than a forward walking preference; that is, pedestrians choose vacant cells in front

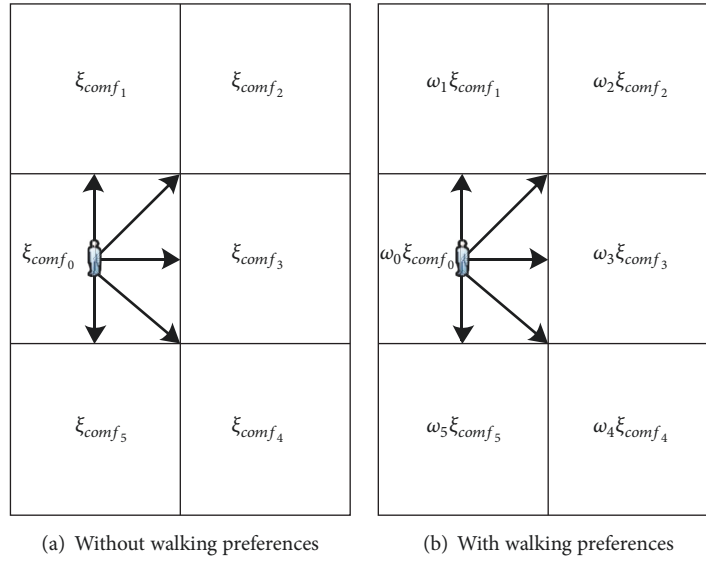


FIGURE 13: Expected comfort utilities for pedestrian choices with/without walking preferences.

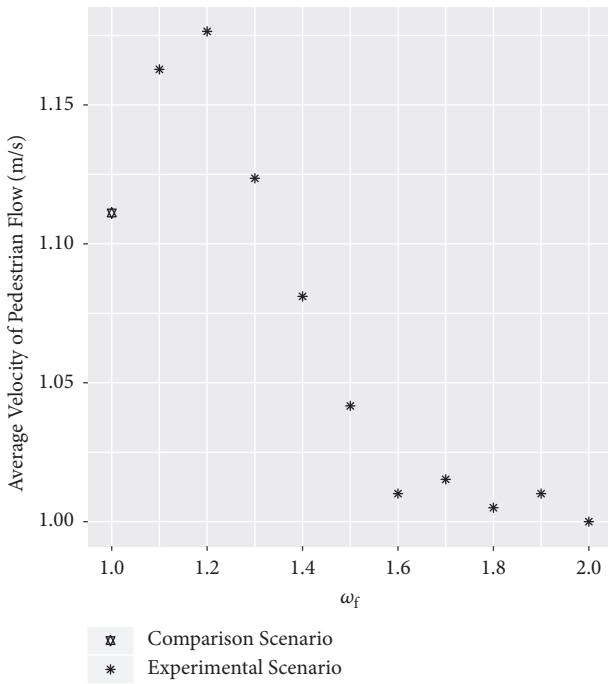


FIGURE 14: Average Velocity of Pedestrian Flow varying over  $\omega_f$ .

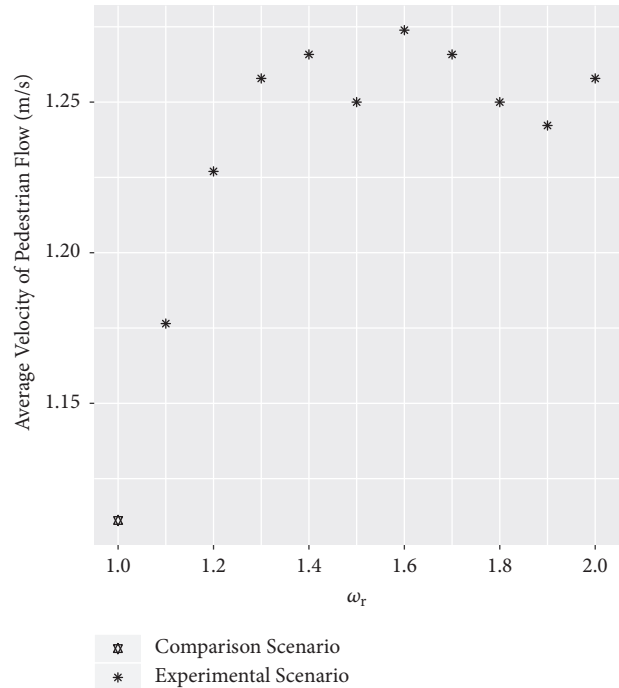


FIGURE 15: Average Velocity of Pedestrian Flow varying over  $\omega_r$ .

first. Therefore, the weight coefficient set  $\omega$  combinations in each right walking preference experiment are shown in Table 5.

Similarly, the pedestrian's right moving preference degree is defined to obey a normal distribution with a mean value  $\omega_r$  and a standard deviation 0.1. It can be found that the pedestrian preference degree to right hand cells increases with  $\omega_r$ . Because of the right walking preference, which keeps bidirectional pedestrians in good order, pedestrians in two directions are divided into two lanes immediately. As a

result, the right walking preference increases AVPF overall, which is different from forward walking preferences. Further, when  $\omega_r \geq 1.4$ , the AVPF fluctuated around 1.26m/s, which indicates that a right walking preference has a limited effect on the AVPF. This is mainly because, with  $\omega_r$  increasing, the right hand side becomes crowded, and the speed is restrained. Figure 15 shows the AVPF changes over  $\omega_r$ .

We thus conclude that it is beneficial for pedestrians to walk on the right (or left) as this separates the bidirectional

TABLE 5: Weight coefficient set in each scenario.

Scenario	The weight coefficient set
Comparison Scenario (No Walking Preferences)	$\omega_0 = \omega_1 = \omega_2 = 1.0, \omega_3 = \omega_4 = \omega_5 = 1.0;$
Experimental Scenarios (Right walking Preferences)	$\omega_0 = \omega_1 = \omega_2 = 1.0, \omega_3 = \omega_4 = \omega_5 \sim N(\omega_r, 0.1^2);$

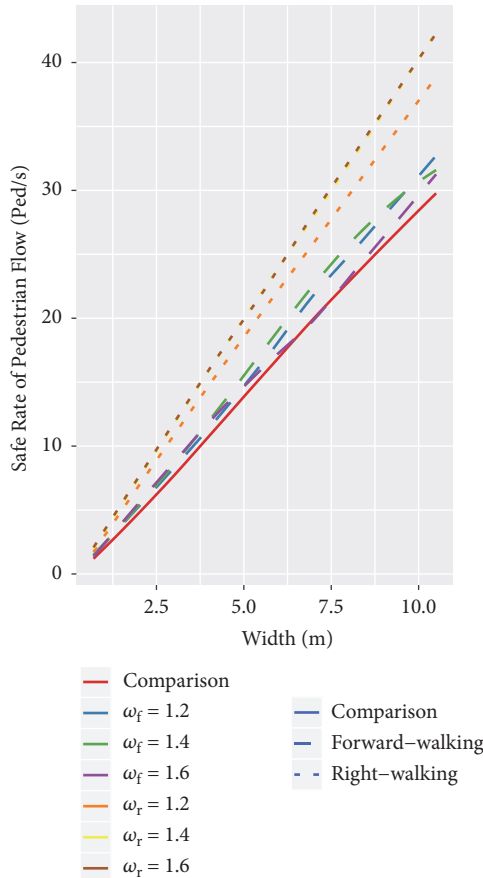


FIGURE 16: Safe rate of pedestrian flow with variances in tunnel width and walking preference.

pedestrians and improves walking speeds. Therefore, by comparing Figures 14 and 15, it can be seen that side walking preferences better improve pedestrian flow efficiency than forward walking preferences.

**5.3. Safe Rate of Pedestrian Flow considering Walking Preferences.** Therefore, it has been proven that both forward walking and side walking preferences influence average pedestrian flow velocity, which can affect the SPFR. To examine this further, simulation experiments over seven scenarios are conducted to explore this effect. The seven scenarios are a comparison scenario (no walking preferences), three forward walking preference scenarios ( $\omega_f = 1.2, 1.4, 1.6$ ), and three side walking scenarios ( $\omega_r = 1.2, 1.4, 1.6$ ). In each scenario, many experiments are conducted to assess the SPFR effect, as shown in Figure 16.

As can be seen in Figure 16, both forward walking and side walking preferences increase the SPFR to some degree. The side walking preference (right) always increased the SPFR; however, the increase is not very obvious when  $\omega_r \geq 1.4$ . In the forward walking preference, the SPFR first increases and then decreases, with the conclusion being that, in consideration of public safety, the SPFR should not exceed that in the comparison scenario; that is,

$$y = 2.9643x - 1.0333 \quad (13)$$

where  $y$  is the SPFR and  $x$  is the tunnel width. In other words, the total flow rate of pedestrians entering a tunnel from both ends should satisfy this relationship for security reasons; that is, the SPFR can increase by 2.96ped/s as the tunnel width expands by 1m.

## 6. Conclusion

This paper studies crowd management by combining a multi-agent system with the Bayesian-Nash Equilibrium. In the model, pedestrians make decisions based on their expected utility, which is calculated through the Bayesian-Nash Equilibrium and their own preferences, and then take collision avoidance actions before moving. The proposed model is calibrated and validated using data collected from a real tunnel. Simulation experiments over multiple scenarios are then conducted. From the experimental data, we find that the Safe Pedestrian Flow Rate increased by 2.96ped/s as the tunnel width expanded by 1m. We also find that both forward walking preferences and side (left or right) walking preferences are able to improve average pedestrian flow velocity, which can be beneficial for the crowd management.

Different from other researches, this paper focuses on mitigating the harmful effects caused by crowd accidents through managing safe pedestrian flows in advance. That is, according to the conclusion, crowd managers can decide how many pedestrians are allowed to go through a tunnel at the same time. Since the emergency management for crowds is a social science, which is mainly based on experience, our work can give references for the managers and be beneficial for the public safety.

However, even at a low pedestrian flow rate, pedestrians may panic in an emergency; therefore, in future research, pedestrian psychology, social relationships, information transmission, and obstacles should be considered for results that are more accurate.

## Data Availability

The data used to support the findings of this study are available from the corresponding author upon request.

## Conflicts of Interest

On behalf of all authors, the corresponding author states that there are no conflicts of interest.

## Acknowledgments

This research is supported by the National Natural Science Foundation of China (No. 71473232, No. 71573237, 71874165), New Century Excellent Talents in University of China (No. NCET-13-1012), Research Foundation of Humanities and Social Sciences of Ministry of Education of China (No. 15YJA630019), China Institute of Geo-Environment Monitoring (No. 0001212016CC60013), and Natural Science Foundation of Hubei Province of China (No. 2016CFB503).

## References

- [1] G. N. Ratty, *Essentials of Autopsy Practice*, Springer International Publishing, Cham, 2017.
- [2] R. L. Hughes, "A continuum theory for the flow of pedestrians," *Transportation Research Part B: Methodological*, vol. 36, no. 6, pp. 507–535, 2002.
- [3] L. Huang, S. C. Wong, M. Zhang, C.-W. Shu, and W. H. K. Lam, "Revisiting Hughes' dynamic continuum model for pedestrian flow and the development of an efficient solution algorithm," *Transportation Research Part B: Methodological*, vol. 43, no. 1, pp. 127–141, 2009.
- [4] Lu. Chunxia, "Analysis on the Wave of Pedestrians," *China Saf. Sci. J.*, vol. 16, no. 2, p. 30, 2006.
- [5] D. Helbing, M. Isobe, T. Nagatani, and K. Takimoto, "Lattice gas simulation of experimentally studied evacuation dynamics," *Physical Review E: Statistical, Nonlinear, and Soft Matter Physics*, vol. 67, no. 6, 2003.
- [6] Y. Han and H. Liu, "Modified social force model based on information transmission toward crowd evacuation simulation," *Physica A: Statistical Mechanics and its Applications*, vol. 469, pp. 499–509, 2017.
- [7] C. Ningbo, W. Wei, Q. Zhaowei, Z. Liying, and B. Qiaowen, "Simulation of Pedestrian Crossing Behaviors at Unmarked Roadways Based on Social Force Model," *Discrete Dynamics in Nature and Society*, vol. 2017, 2017.
- [8] L. A. Pereira, D. Burgarelli, L. H. Duczmal, and F. R. B. Cruz, "Emergency evacuation models based on cellular automata with route changes and group fields," *Physica A: Statistical Mechanics and its Applications*, vol. 473, pp. 97–110, 2017.
- [9] H. Yue, H. Guan, J. Zhang, and C. Shao, "Study on bi-direction pedestrian flow using cellular automata simulation," *Physica A: Statistical Mechanics and its Applications*, vol. 389, no. 3, pp. 527–539, 2010.
- [10] B. Basak and S. Gupta, "Developing an agent-based model for pilgrim evacuation using visual intelligence: A case study of Ratha Yatra at Puri," *Computers, Environment and Urban Systems*, vol. 64, pp. 118–131, 2017.
- [11] N. Wagner and V. Agrawal, "An agent-based simulation system for concert venue crowd evacuation modeling in the presence of a fire disaster," *Expert Systems with Applications*, vol. 41, no. 6, pp. 2807–2815, 2014.
- [12] N. Wijermans, C. Conrado, M. van Steen, C. Martella, and J. Li, "A landscape of crowd-management support: An integrative approach," *Safety Science*, vol. 86, pp. 142–164, 2016.
- [13] H. Vermuyten, J. Beliën, L. De Boeck, G. Reniers, and T. Wauters, "A review of optimisation models for pedestrian evacuation and design problems," *Safety Science*, vol. 87, pp. 167–178, 2016.
- [14] V. J. Kok, M. K. Lim, and C. S. Chan, "Crowd behavior analysis: A review where physics meets biology," *Neurocomputing*, vol. 177, pp. 342–362, 2016.
- [15] D. C. Duives, W. Daamen, and S. P. Hoogendoorn, "State-of-the-art crowd motion simulation models," *Transportation Research Part C: Emerging Technologies*, vol. 37, pp. 193–209, 2014.
- [16] J. Yuen, E. Lee, and W. Lam, "An intelligence-based route choice model for pedestrian flow in a transportation station," *Applied Soft Computing*, vol. 24, pp. 31–39, 2014.
- [17] A. Borrmann, A. Kneidl, G. Köster, S. Ruzika, and M. Thiemann, "Bidirectional coupling of macroscopic and microscopic pedestrian evacuation models," *Safety Science*, vol. 50, no. 8, pp. 1695–1703, 2012.
- [18] M. Zhou, H. Dong, F.-Y. Wang, Q. Wang, and X. Yang, "Modeling and simulation of pedestrian dynamical behavior based on a fuzzy logic approach," *Information Sciences*, vol. 360, pp. 112–130, 2016.
- [19] M. Kaji and T. Inohara, "Cellular automaton simulation of unidirectional pedestrians flow in a corridor to reproduce the unique velocity profile of Hagen–Poiseuille flow," *Physica A: Statistical Mechanics and its Applications*, vol. 467, pp. 85–95, 2017.
- [20] G. H. Goldsztein, "Crowd of individuals walking in opposite directions. A toy model to study the segregation of the group into lanes of individuals moving in the same direction," *Physica A: Statistical Mechanics and its Applications*, vol. 479, pp. 162–173, 2017.
- [21] Lili Lu, Gang Ren, Wei Wang, Chen Yu, and Chenzi Ding, "Exploring the Effects of Different Walking Strategies on Bi-Directional Pedestrian Flow," *Discrete Dynamics in Nature and Society*, vol. 2013, Article ID 150513, 9 pages, 2013.
- [22] S. Ye, L. Wang, K. H. Cheong, and N. Xie, "Pedestrian Group-Crossing Behavior Modeling and Simulation Based on Multidimensional Dirty Faces Game," *Complexity*, vol. 2017, Article ID 1723728, 12 pages, 2017.
- [23] A. Abdelghany, K. Abdelghany, H. Mahmassani, and W. Alhalabi, "Modeling framework for optimal evacuation of large-scale crowded pedestrian facilities," *European Journal of Operational Research*, vol. 237, no. 3, pp. 1105–1118, 2014.
- [24] J. Guan, K. Wang, and F. Chen, "A cellular automaton model for evacuation flow using game theory," *Physica A: Statistical Mechanics and its Applications*, vol. 461, pp. 655–661, 2016.
- [25] M. Tang, H. Jia, B. Ran, and J. Li, "Analysis of the pedestrian arching at bottleneck based on a bypassing behavior model," *Physica A: Statistical Mechanics and its Applications*, vol. 453, pp. 242–258, 2016.
- [26] B. L. Mesmer and C. L. Bloebaum, "Modeling decision and game theory based pedestrian velocity vector decisions with interacting individuals," *Safety Science*, vol. 87, pp. 116–130, 2016.
- [27] N. Guo, Q.-Y. Hao, R. Jiang, M.-B. Hu, and B. Jia, "Uni- and bi-directional pedestrian flow in the view-limited condition: Experiments and modeling," *Transportation Research Part C: Emerging Technologies*, vol. 71, pp. 63–85, 2016.
- [28] R. A. Kady, "The development of a movement-density relationship for people going on four in evacuation," *Safety Science*, vol. 50, no. 2, pp. 253–258, 2012.

- [29] M. Haghani and M. Sarvi, "Stated and revealed exit choices of pedestrian crowd evacuees," *Transportation Research Part B: Methodological*, vol. 95, pp. 238–259, 2017.
- [30] L. Lu, C.-Y. Chan, J. Wang, and W. Wang, "A study of pedestrian group behaviors in crowd evacuation based on an extended floor field cellular automaton model," *Transportation Research Part C: Emerging Technologies*, vol. 81, pp. 317–329, 2017.
- [31] G. Zhang, D. Huang, G. Zhu, and G. Yuan, "Probabilistic model for safe evacuation under the effect of uncertain factors in fire," *Safety Science*, vol. 93, pp. 222–229, 2017.
- [32] K. Huang and X. Zheng, "A weighted evolving network model for pedestrian evacuation," *Applied Mathematics and Computation*, vol. 298, pp. 57–64, 2017.
- [33] L. Fu, W. Song, and S. Lo, "A fuzzy-theory-based method for studying the effect of information transmission on nonlinear crowd dispersion dynamics," *Communications in Nonlinear Science and Numerical Simulation*, vol. 42, pp. 682–698, 2017.
- [34] Y. Li, H. Liu, G.-P. Liu, L. Li, P. Moore, and B. Hu, "A grouping method based on grid density and relationship for crowd evacuation simulation," *Physica A: Statistical Mechanics and its Applications*, vol. 473, pp. 319–336, 2017.
- [35] F. Guo, X. Li, H. Kuang, Y. Bai, and H. Zhou, "An extended cost potential field cellular automata model considering behavior variation of pedestrian flow," *Physica A: Statistical Mechanics and its Applications*, vol. 462, pp. 630–640, 2016.
- [36] S. Li, J. Zhuang, S. Shen, and J. Wang, "Driving-forces model on individual behavior in scenarios considering moving threat agents," *Physica A: Statistical Mechanics and its Applications*, vol. 481, pp. 127–140, 2017.
- [37] X. Li, F. Guo, H. Kuang, and H. Zhou, "Effect of psychological tension on pedestrian counter flow via an extended cost potential field cellular automaton model," *Physica A: Statistical Mechanics and its Applications*, vol. 487, pp. 47–57, 2017.
- [38] C. von Krüchten and A. Schadschneider, "Empirical study on social groups in pedestrian evacuation dynamics," *Physica A: Statistical Mechanics and its Applications*, vol. 475, pp. 129–141, 2017.
- [39] Y. Han, H. Liu, and P. Moore, "Extended route choice model based on available evacuation route set and its application in crowd evacuation simulation," *Simulation Modelling Practice and Theory*, vol. 75, pp. 1–16, 2017.
- [40] G. Zeng, S. Cao, C. Liu, and W. Song, "Experimental and modeling study on relation of pedestrian step length and frequency under different headways," *Physica A: Statistical Mechanics and its Applications*, vol. 500, pp. 237–248, 2018.

